Pergamon

PII: S0277-5387(97)00195-2

Polyhedron Vol. 16, No. 23, pp. 3953–3966, 1997
© 1997 Elsevier Science Ltd
All rights reserved. Printed in Great Britain
0277-5387/97 $17.00+0.00

X-ray crystal structures and Mössbauer studies of some trismalonatoferrate(III) compounds

S. Calogero,[a]* L. Stievano,[a] L. Diamandescu,[b] D. Mihăilă-Tărăbăşanu[b] and G. Valle[c]

[a]Dipartimento di Chimica Fisica, Università, I-30123 Venezia, Italy

[b]Institute of Atomic Physics, P.O. Box MG-6, Bucharest, Romania

[c]Centro di Studio dei Biopolimeri del CNR, Università, I-35100 Padova, Italy

(Received 6 March 1997; accepted 13 May 1997)

Abstract—Three trismalonatoferrate compounds (20% enriched in ^{57}Fe) NaBa $(FeMa_3)\cdot 3H_2O$ (**1**), $[Na_3(FeMa_3)]_2\cdot 8H_2O$ (**2**), and $Na_3(FeMa_3)\cdot 8H_2O\cdot\frac{1}{2}Sol$ (**3**) (Ma is the malonato anion and Sol is a solvate molecule) have been prepared and their X-ray crystal structures determined. The Mössbauer spectra exhibit a broadened line at 293 and 4.2 K indicating the presence of spin relaxation effects. The spectra data, fitted following Afanas'ev and Wickman models, point to the presence of spin–spin isotropic relaxation mechanism.
© 1997 Elsevier Science Ltd

Keywords: Malonatoferrate; crystal structure; Mössbauer spectroscopy; relaxation; Afanas'ev theory; Wickman theory; enriched iron.

Due to the strong affinity of iron(III) for oxygen donor ligands, the iron(III) complexes are particularly important in biological systems. In addition photosensitive iron(III) complexes have been used in non silver photographic processes and some others could be used as raw materials in the field of ceramic products [1,2].

Malonic acid forms with iron(III), the trismalonato anion analogous to that obtained starting with oxalic acid. Lithium, potassium, sodium, rubidium, caesium, ammonium, and thallium salts, of colour variable from yellow–green to emerald–green, are known [3]. They are relatively stable in aqueous solutions even if the malonato compounds, involving six-atom rings, are presumably less stable than the oxalato ones involving five-atom chelate rings [4]. In fact the malonates show a spontaneous decomposition of malonic acid to carbon dioxide and acetic acid.

During the last 10 years, the malonato compounds have been the subject of many investigations [5–10]. Abras [7] and Bassi [5] have studied alkali trismalonato ferrates(III); they reported broadened Mössbauer spectra with unusually large linewidth which could not be fitted to any combination of two Lorentzian lines. A similar behaviour has been observed in a series of trisoxalatoferrate(III) complexes [11–13] that were analysed in terms of electronic relaxation effects by Mössabauer spectroscopy. Due to the presence of the CH_2 group in trismalonatos it would be particularly interesting to see how this increased carbon chain affects the electronic properties of the iron(III) complexes having malonates as ligands. This prompted us to initiate a structural and Mössbauer study of sodium-barium trismalonatoferrate (**1**), sodium trismalonatoferrate (**2**) together with a solvate sodium trismalonatoferrate (**3**).

EXPERIMENTAL

Sodium–barium trismalonatoferrate trihydrate (**1**)

Compound **1** was synthesised by digesting a mixture of iron(III) sulfate (6 mmol), sodium malonate (0.15 mmol), and barium malonate (0.22 mmol) in distilled water (50 ml) at room temperature under stirring for 1 h. After filtration green crystals grew out of the solution by slow evaporation. The starting iron(III)

* Author to whom correspondence should be addressed.

sulphate was prepared by dissolving metallic ^{57}Fe in 25% sulphuric acid on water bath. After evaporation the enriched iron(III) sulphate was dissolved and then crystallized from water.

Sodium trismalonatoferrate octahydrate (**2**)

Compound **2** was obtained by adding the stoichiometric quantity of sodium malonate in water to a solution of iron(III) sulphate (0.4 M) (20% enriched in ^{57}Fe). After removing sodium sulphate, green crystals of the compound **2** were grown from the solution by slow evaporation at room temperature.

Sodium trismalonatoferrate octahydrate (**3**)

Compound **3** was prepared by adding the stoichiometric amount of sodium malonate solution to an iron nitrate solution (0.4 M). After removing sodium nitrate, a few ml of dioxane were added. The green crystals were grown from the water–dioxane solution by slow evaporation under low vacuum.

X-ray crystal procedure

Intensity data were measured at room temperature with a Philips PW 1100 diffractometer using Mo-K_α radiation. The intensities were corrected for Lorentz-polarisation effects and for absorption. Crystal data, data collection, and refinement parameters are listed in Table 1. The structures were solved by direct methods using the SHELXS 86 program. Blocked full-matrix least-squares refinement on F minimised the function $\Sigma w[|F_o| - |F_c|]^2$. The non-hydrogen atoms were refined anisotropically. The position of the hydrogen atoms were calculated but not refined. General views of compounds **1**, **2** and **3** are displayed together with their atomic numbering schemes in Figs 1, 2 and 3, respectively.

X-ray crystal analyses showed that **1** is NaBa $(FeMa_3)\cdot 3H_2O$, **2** is $[Na_3(FeMa_3)]_2\cdot 8H_2O$ and **3** is $Na_3(FeMa_3)\ 8H_2O\cdot\frac{1}{2}Sol$ (where Ma is the malonato anion $CO_2CH_2CO_2$, and Sol is a solvant molecule). Selected bond distances and angles are reported in Tables 2–4 for **1**, in Tables 5–7 for **2**, and in Tables 8–10 for **3**. The dihedral angles between weighted least-squares planes for the compounds **1**, **2** and **3** are reported in Table 11. The final atomic coordinates have been deposited with the Editor together with anisotropic thermal parameters, the coordinates of H atoms and structure factors.

Mössbauer spectroscopy

Polycrystalline samples were prepared by grinding single crystals (20% enriched in ^{57}Fe). Both $^{57}Co/Rh$ source and absorber were kept at room temperature or at the liquid helium temperature. A sinusoidal velocity waveform and a proportional detector were used. The spectra were fitted by various relaxation models [14,15] using computer programs. The hyperfine parameters, in mm/s, such as isomer shift IS (relative to metallic iron), quadrupole splitting QS, and linewidth LW, are listed in Table 12 together with the relaxation

Table 1. Crystallographic data

Compound	**1**	**2**	**3**
Formula	$C_9H_{12}FeNaBaO_{15}$	$C_{18}H_{28}Fe_2Na_6O_{32}$	$C_{24}H_{44}Fe_2Na_8O_{44}$
M	576	1006	1332
Crystal system	Monoclinic	Triclinic	Triclinic
Space group	$P2_1/n$ (No. 14)	$P\bar{1}$ (No. 2)	$P\bar{1}$ (No. 2)
Crystal size/mm	$0.2\times0.6\times0.4$	$0.6\times0.6\times0.4$	$0.3\times0.3\times0.5$
a (Å)	11.113(2)	14.497(2)	11.395(1)
b (Å)	13.512(2)	14.758(2)	11.970(1)
c (Å)	10.276(2)	9.148(1)	9.995(1)
α (°)		91.0(1)	101.2(1)
β (°)	90.8(1)°	105.4(1)	90.8(1)
		67.6(1)	63.5(1)
U (Å^3)	1542.9(5)	1736.0(2)	1192.7(1)
Z	4	2	1
D_c (g cm^{-3})	2.48	1.92	1.85
μ (Mo-K_α)/cm^{-1}	33.71	10.20	7.98
Data collection range	$4.7 < 2\vartheta < 56.0$	$6.5 < 2\vartheta < 120.0$	$4.0 < 2\vartheta < 56.0$
No. unique reflections	3910	5185	5757
Data with $F > 3\sigma(F)$	2902	4599	4911
$F(000)$	1116	1020	680
R	0.045	0.056	0.067
R_w	0.046	0.059	0.069

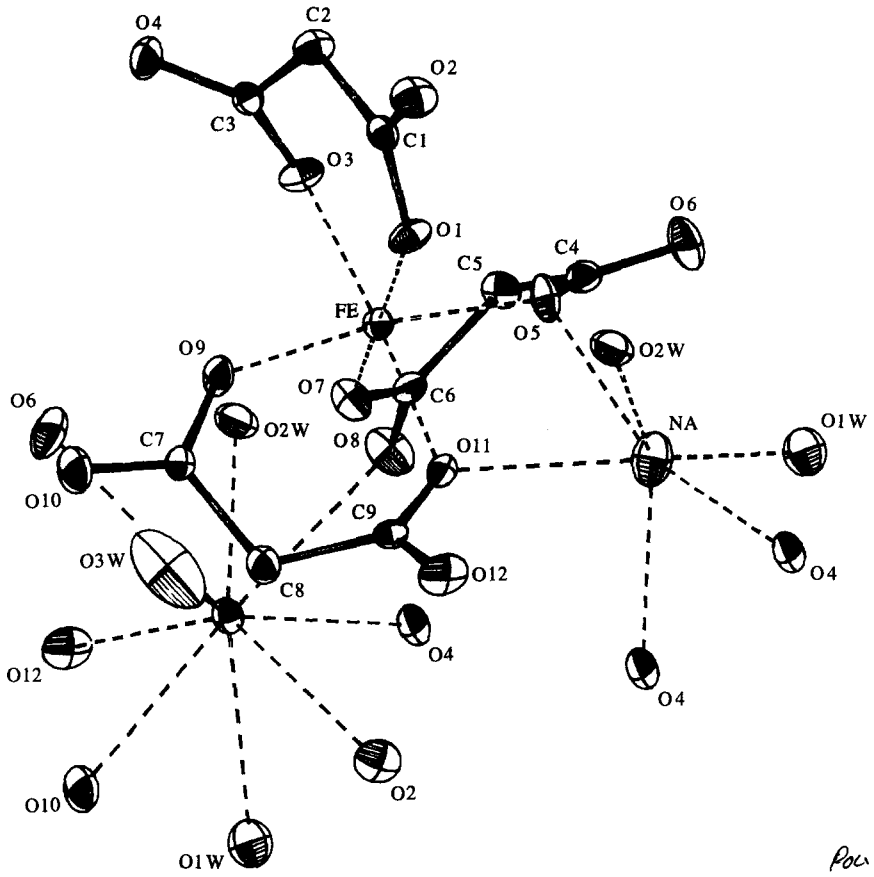

Fig. 1. ORTEP plot for sodium-barium trismalonatoferrate trihydrate (**1**).

parameters (the tensor γ in s/mm and the relaxation time τ in ns) and the statistic value χ^2.

RESULTS AND DISCUSSION

Molecular structure of sodium–barium trismalonatoferrate trihydrate (**1**)

As shown in Fig. 1, three metallic sites are present in $NaBa[FeMa_3]\cdot 3H_2O$ (**1**): the hexacoordinate iron and sodium environments and the nine coordinate barium cation. In Table 2 the bond distances around the metallic sites are ordered following increasing lengths. The slightly distorted octahedral coordination around iron is formed by six oxygen atoms from the malonate moieties. The sodium site is formed by the oxygen atoms O(4), O(5) and O(11) from different malonate rings together with the oxygen atoms O(1)W and O(2)W from water. The tricapped trigonal prism around the barium cation is achieved by six carbonyl oxygens from three malonate moieties and by three oxygens from water.

All the oxygen atoms of the malonate rings are involved in bonds: the non carbonylic ones around the iron(III) centre and the carbonylic ones around sodium and barium cations. The water oxygens enter in the coordination sphere of sodium and barium cations. In addition the water oxygens O(1)W or O(3)W and one of the malonate oxygen atoms O(3), O(6), O(7) and O(12) form five possible hydrogen bonds (Table 4). The packing of the structure is substantially due to the presence of the water molecules.

Molecular structure of sodium trismalonatoferrate octahydrate (**2**)

As shown in Fig. 2, the compound $\{Na_3[FeMa_3]\}_2\cdot 8H_2O$ (**2**) contains two distinct octahedral iron (III) sites with oxygen ligands from malonate moieties and seven sodium sites with carbonyl oxygens from malonato rings or from water. Since the site occupancy of Na(1) and Na(2) is 0.5 the molecule contains six sodium atoms. The two slightly distorted iron octahedra are similar in bond lengths and angles (Tables 5 and 6). The sodium sites are hexacoordinate except for Na(7) which is pentacoordinate. Table 5 displays the nature of the oxygen atoms involved in the coordination. It is interesting to note that in the compound **2** the oxygen from water molecules not only enters in the coordination spheres of all the

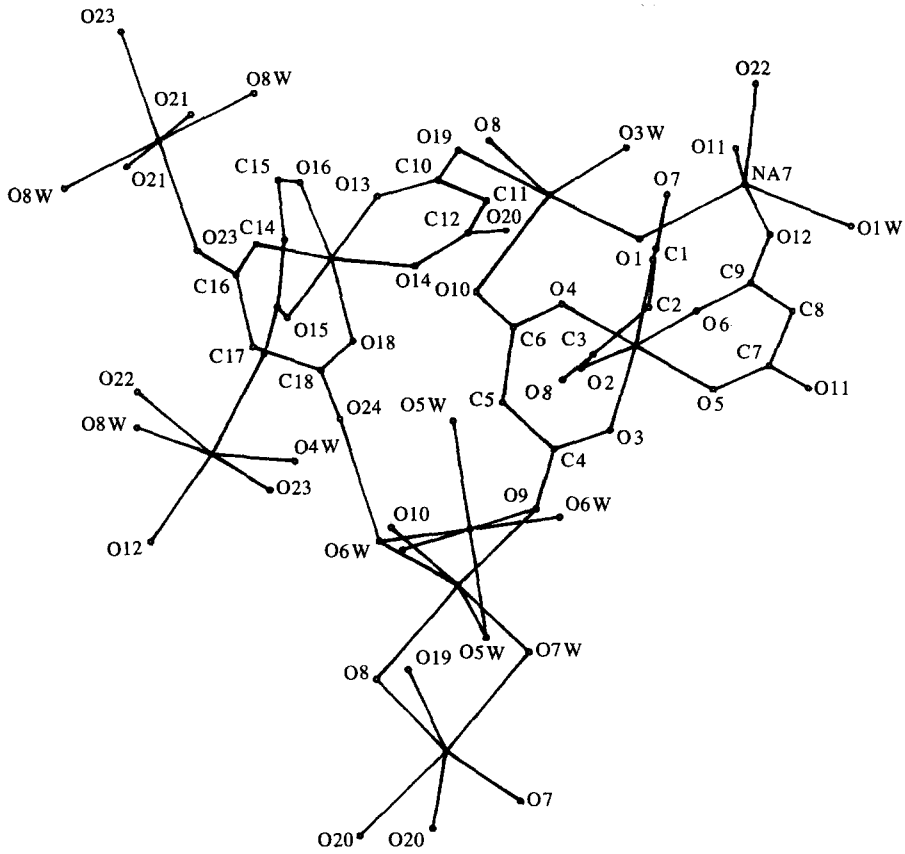

Fig. 2. General view for sodium trismalonatoferrate octahydrate (**2**).

sodium sites but also determines some hydrogen bonds between two water oxygens. This is shown in Table 7 where the complex net of the possible hydrogen bonds, due to the eight water oxygens and other oxygen atoms, is listed. Analogously to the compound **1** the presence of the water molecules is essential for the stability of the compound **2**.

Molecular structure of the solvate compound (**3**)

The ORTEP plot of Fig. 3a shows that the compound $Na_3(FeMa_3)\cdot 8H_2O\cdot\frac{1}{2}Sol$ (**3**) contains one iron(III) site. The general view of Fig. 3b shows that in addition the molecule contains four octahedral sodium sites and a disordered solvate molecule, not identified, probably due to a rearrangement of decomposition products. Selected bond lengths and angles are reported in Table 8 and 9, respectively.

The Na(1) cation is coordinated to six oxygen atoms: three from one malonato moiety, one from another malonato moiety and two water oxygens. Na(2) is coordinated to four oxygens from water and the oxygen atoms O(7) and O(7, $-x+1, -y, -z+1$). The cation Na(3) is coordinated to four oxygens from water, the oxygen O(7) from the malonato ring and the oxygen O(2)S from the solvate molecule. Na(4) is coordinated to two oxygens from water, the oxygens O(3) and O(12) from malonate rings and the oxygens O(1)S and O(2)S from the solvate molecule.

The not identified solvate molecule has a symmetry centre at $(-x-1, -y+1, -z)$. The molecule is connected to the cations Na(3) and Na(4) and by hydrogen bonding to the oxygens from water O(1)W and O(8)W. The ten possible hydrogen bonds between oxygens from water and oxygen atoms from malonates and water molecules are listed in Table 10. In addition water molecules enter in the coordination sphere of all the sodium cations, on the contrary of the solvate molecules which interact only with the Na(3) and Na(4) sites. As a result the packing in the compound **3** is due to both water and solvate molecules.

Mössbauer results

As shown in Figs 4 and 5, the Mössbauer spectra of the compounds **1** and **2**, collected both at room and at the liquid helium temperature, consist in a strongly broadened line whose linewidth is about 1.9 mm/s. Since the Mössbauer data for compound **3** are

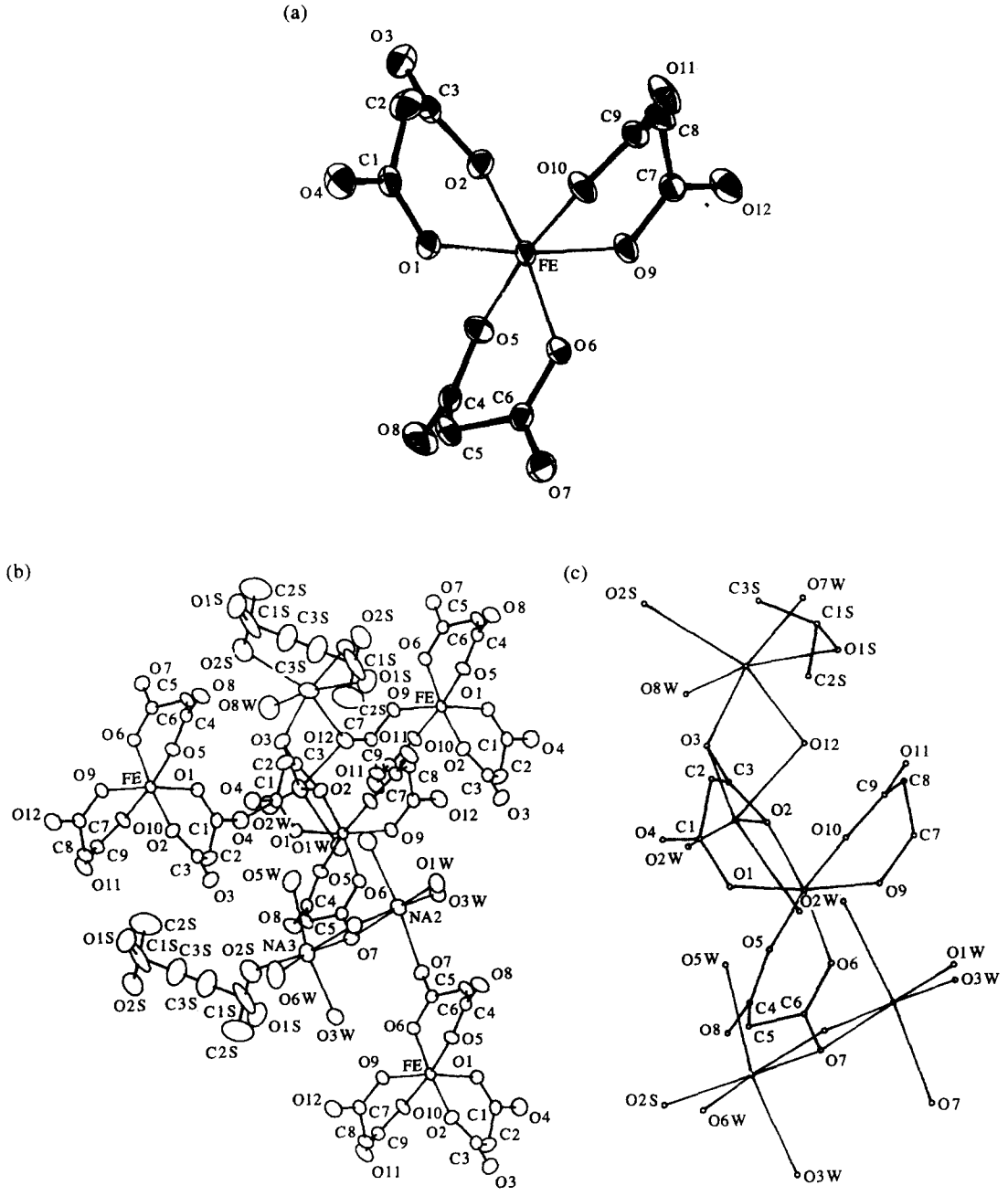

Fig. 3. (a) ORTEP plot for the solvate compound sodium trismalonatoferrate octahydrate (**3**); (b) General view for the solvate compound sodium trismalonatoferrate octahydrate (**3**); (c) The sodium sites in the solvate compound sodium trismalonatoferrate octahydrate (**3**).

expected very similar to those of **2**, the same considerations can be performed for both the compounds. Even if the fit in the hypothesis of a single Lorentzian line is rather bad, the isomer shift values of Table 12 for the compounds **1** and **2** are consistent with the presence of high-spin iron(III) sites. The high spin character of these compounds has been also confirmed by EPR and magnetic susceptibility measurements. Since the two iron sites in the compound **2** are similar (cf. Table 5 and 6) only one spectral component is observed in its Mössbauer spectrum.

On the contrary of the trisoxalatoferrate analogous [16], the weighted least-squares planes FeOCCCO is trismalonatoferrate deviate as expected, significantly from the planarity (cf. Table 11). The mean O—Fe—O angle in the range 87–88° suggests that the larger chelate ring size leads to a slightly less distorted iron site in the Na and NaBa malonates than in pot-

Table 2. Selected bond distances (Å) for $NaBa(FeMa_3)\cdot 3H_2O$ (**1**)

Fe Site			
Fe—O(1)	1.957(3)		
Fe—O(9)	1.962(3)		
Fe—O(7)	1.970(3)		
Fe—O(3)	1.974(3)		
Fe—O(5)	1.980(3)		
Fe—O(11)	1.985(3)		
Na Site		Ba Site	
Na···O(1)W	2.333(4)	Ba···O(12; $x, y, z-1$)	2.667(4)
Na···O(2)W($x+2, y, z$)	2.347(4)	Ba···O(2; $-x+3/2, y-1/2, -z+3/2$)	2.669(3)
Na···O(11)	2.361(4)	Ba···O(8)	2.718(4)
Na···O(4; $x+1/2, -y+1/2, z+1/2$)	2.479(4)	Ba···O (10; $x+1, -y, -z+1$)	2.720(3)
Na···O(4; $-x+3/2, y-1/2, -z+3/2$)	2.518(4)	Ba···O(2)W($x+2, y, z-1$)	2.805(3)
Na···O(5)	2.636(4)	Ba···O(3)W	2.870(6)
		Ba···O(6; $x-1/2, -y+1/2, z-1/2$)	2.871(4)
		Ba···O(1)W($-x+2, -y, -z+1$)	2.912(4)
		Ba···O(4; $x+1/2, -y+1/2, z-1/2$)	2.939(4)

Malonate Rings					
C(1)—C(2)	1.503(6)	C(4)—C(5)	1.494(7)	C(7)—C(8)	1.493(6)
C(2)—C(3)	1.501(6)	C(5)—C(6)	1.503(6)	C(8)—C(9)	1.496(7)
O(1)—C(1)	1.269(5)	O(5)—C(4)	1.273(6)	O(9)—C(7)	1.257(5)
O(2)—C(1)	1.214(5)	O(6)—C(4)	1.227(5)	O(10)—C(7)	1.228(5)
O(3)—C(3)	1.276(5)	O(7)—C(6)	1.264(5)	O(11)—C(9)	1.266(5)
O(4)—C(3)	1.235(5)	O(8)—C(6)	1.227(5)	O(12)—C(9)	1.219(6)

Table 3. Selected bond angles (°) for $NaBa(FeMa_3)\cdot 3H_2O$ (**1**)

Fe Site		Na and Ba Sites	
O(5)—Fe—O(11)	85.3(2)	O(5)—Na—O(11)	64.8(1)
O(5)—Fe—O(7)	86.6(2)	O(3)W—Ba—O(8)	75.1(1)
O(3)—Fe—O(9)	87.2(2)	O(1)W—Na—O(5)	85.1(2)
O(1)—Fe—O(11)	87.5(1)	O(1)W—Na—O(11)	136.1(2)
O(1)—Fe—O(3)	87.8(1)		
O(7)—Fe—O(9)	88.8(2)		
O(3)—Fe—O(7)	88.9(1)		
O(1)—Fe—O(5)	90.3(2)		
O(1)—Fe—O(9)	94.7(2)		
O(7)—Fe—O(11)	96.1(1)		

Malonate Rings					
C(1)—C(2)—C(3)	118.8(3)	C(4)—C(5)—C(6)	116.9(4)	C(7)—C(8)—C(9)	117.1(4)
O(2)—C(1)—C(2)	117.9(4)	O(6)—C(4)—C(5)	118.3(4)	O(11)—C(9)—C(8)	117.4(4)
O(3)—C(3)—C(2)	117.9(4)	O(7)—C(6)—C(5)	118.3(4)	O(10)—C(7)—C(8)	118.5(4)
O(1)—C(1)—C(2)	118.9(4)	O(5)—C(4)—C(5)	118.9(4)	O(12)—C(9)—C(8)	119.1(4)
O(4)—C(3)—C(2)	119.1(4)	O(8)—C(6)—C(5)	119.3(4)	O(9)—C(7)—C(8)	119.3(4)
O(3)—C(3)—O(4)	122.9(4)	O(7)—C(6)—O(8)	122.3(4)	O(9)—C(7)—O(10)	122.2(4)
O(1)—C(1)—O(2)	123.2(4)	O(5)—C(4)—O(6)	122.8(4)	O(11)—C(9)—O(12)	123.4(5)

assium trisoxalato complex where the angle is 85° [17]. However, the greater steric hindrance in malonates in comparison with analogous oxalates does not influence very much the closest Fe···Fe distance (Table 11) which is comparable to that reported for oxalates. That means the dipole–dipole and exchange interaction between iron atoms and consequently the intensity of spin relaxation must be of the same order of magnitude in both systems. The line broadening of Mössbauer spectra of the studied malonates could be caused by the expected electronic spin relaxation [11,15].

It was shown by Afanas'ev and Gorobchenco [14] that, in the case of fast relaxation limit, the Mössbauer line shape can be described by a sum of Lorentzian lines whose intensities and widths can be easily

Table 4. Possible hydrogen bonds (Å) and angles (°) for $NaBa(FeMa_3)\cdot 3H_2O$ (1)

D—H···A[a]	D—H	D···A	H···A	Angle
O(3)—H(1)W(3)···O(7)(*i*)	1.191(6)	2.803(7)	1.660(3)	158.6(3)
O(1)W—H(1)W(1)···O(3)(*ii*)	1.190(4)	2.962(5)	1.933(3)	141.8(3)
O(1)W—H(2)W(1)···O(6)(*i*)	0.971(4)	2.991(5)	2.176(4)	140.7(3)
O(1)W—H(1)W(1)···O(12)(*iii*)	1.190(4)	3.002(5)	2.396(3)	108.9(2)
O(3)W—H(2)W(3)···O(6)(*iv*)	1.181(6)	3.008(6)	2.071(4)	133.4(3)

[a] Equivalent positions (*i*) x, y, z (*ii*) $x+1/2, -y+1/2, z+1/2$ (*iii*) $-x+2, -y, -z+2$ (*iv*) $x-1/2, -y+1/2, z-1/2$.

Table 5. Selected bond distances (Å) for $[Na_3(FeMa_3)]_2\cdot 8H_2O$ (2)

Fe(1) Site		Fe(2) Site			
Fe(1)—O(3)	1.968(6)	Fe(2)—O(17)	1.976(8)		
Fe(1)—O(4)	1.969(7)	Fe(2)—O(14)	1.983(8)		
Fe(1)—O(6)	1.987(5)	Fe(2)—O(18)	1.995(6)		
Fe(1)—O(5)	1.994(6)	Fe(2)—O(13)	2.002(6)		
Fe(1)—O(1)	2.021(6)	Fe(2)—O(15)	2.006(6)		
Fe(1)—O(2)	2.045(6)	Fe(2)—O(16)	2.011(6)		
Na(1) Site[a]				Na(2) Site[b]	
Na(1)···O(6)W		2.286(9)		Na(2)···O(21; $-x-1, -y+2, -z$)	2.388(6)
Na(1)···O(5)W		2.339(6)		Na(2)···O(8)W	2.415(8)
Na(1)···O(9; $-x, -y+1, -z$)		2.518(6)		Na(2)···O(23; $-x-1, -y+2, -z+1$)	2.556(7)
Na(3) Site				Na(4) Site	
Na(3)···O(10; $-x, -y+1, -z+1$)		2.351(8)		Na(4)···O(7; $x, y-1, z$)	2.345(6)
Na(3)···O(7)W($-x, -y+1, -z+1$)		2.380(7)		Na(4)···O(19; $-x, -y+1, -z+1$)	2.407(7)
Na(3)···O(9)		2.410(9)		Na(4)···O(20; $-x, -y+1, -z$)	2.409(7)
Na(3)···O(6)W		2.420(7)		Na(4)···O(8; $-x, -y+1, -z$)	2.461(6)
Na(3)···O(5)W		2.512(8)		Na(4)···O(20; $x, y-1, z$)	2.581(9)
Na(3)···O(8; $-x, -y+1, -z$)		2.527(8)		Na(4)···O(7)W($-x, -y+1, -z+1$)	2.638(9)
Na(5) Site		Site		Na(7) Site	
Na(5)···O(4)W	2.385(7)	Na(6)···O(3)W	2.279(1)	Na(7)···O(11; $x, y, z+1$)	2.295(9)
Na(5)···O(12; $x-1, y, z-1$)	2.397(9)	Na(6)···O(8; $-x, -y+1, -z+1$)	2.399(7)	Na(7)···O(12)	2.353(8)
Na(5)···O(23; $x, y, z-1$)	2.400(9)	Na(6)···O(19)	2.418(7)	Na(7)···O(22; $-x, -y+2, -z+1$)	2.368(9)
Na(5)···O(21)	2.417(9)	Na(6)···O(4)	2.477(7)	Na(7)···O(1)W($x, y, z+1$)	2.416(8)
Na(5)···O(8)W($-x-1, -y+2, -z$)	2.434(7)	Na(6)···O(10)	2.487(9)	Na(7)···O(2)W	2.465(9)
Na(5)···O(22; $-x-1, -y+2, -z$)	2.727(9)	Na(6)···O(2)W	2.497(7)		
Malonate Rings					
C(11)—C(12)	1.48(1)	C(13)—C(14)	1.49(1)	C(16)—C(17)	1.48(2)
C(1)—C(2)	1.51(1)	C(4)—C(5)	1.49(1)	C(7)—C(8)	1.49(1)
C(10)—C(11)	1.51(2)	C(14)—C(15)	1.51(1)	C(17)—C(18)	1.52(2)
C(2)—C(3)	1.52(1)	C(5)—C(6)	1.54(1)	C(8)—C(9)	1.53(1)
O(19)—C(10)	1.22(9)	O(10)—C(6)	1.22(1)	O(11)—C(7)	1.20(1)
O(20)—C(12)	1.23(1)	O(9)—C(4)	1.26(1)	O(12)—C(9)	1.22(1)
O(7)—C(1)	1.23(1)	O(3)—C(4)	1.26(1)	O(23)—C(16)	1.23(1)
O(14)—C(12)	1.27(1)	O(16)—C(15)	1.26(1)	O(18)—C(18)	1.24(1)
O(2)—C(3)	1.28(1)	O(21)—C(13)	1.26(1)	O(17)—C(16)	1.25(1)
O(13)—C(10)	1.28(1)	O(15)—C(13)	1.27(1)	O(5)—C(7)	1.28(1)
O(1)—C(1)	1.28(1)	O(4)—C(6)	1.28(1)	O(6)—C(9)	1.30(1)

[a] Site occupancy 0.5 in special position (0, 1/2, 0)

[b] Site occupancy 0.5 in special position (−1/2, 1, −1/2).

Table 6. Selected bond angles (°) for $[Na_3(FeMa_3)]_2 \cdot 8H_2O$ (**2**)

Fe(1) Site			
O(1)—Fe(1)—O(6)	85.6(3)	O(3)—Fe(1)—O(4)	88.1(4)
O(5)—Fe(1)—O(6)	86.4(3)	O(2)—Fe(1)—O(3)	88.8(3)
O(3)—Fe(1)—O(5)	89.4(3)	O(4)—Fe(1)—O(6)	89.5(3)
O(1)—Fe(1)—O(4)	90.8(3)	O(2)—Fe(1)—O(5)	90.4(3)
O(2)—Fe(1)—O(4)	94.2(3)	O(1)—Fe(1)—O(5)	92.3(4)
Fe(2) Site			
O(13)—Fe(2)—O(17)	84.5(3)	O(17)—Fe(2)—O(18)	88.2(3)
O(15)—Fe(2)—O(16)	86.7(3)	O(16)—Fe(2)—O(17)	88.4(4)
O(15)—Fe(2)—O(18)	87.1(3)	O(13)—Fe(2)—O(16)	90.7(3)
O(14)—Fe(2)—O(15)	90.2(3)	O(14)—Fe(2)—O(18)	92.0(4)
O(13)—Fe(2)—O(18)	95.7(3)	O(14)—Fe(2)—O(16)	92.2(4)
Na Sites			
O(9)—Na(1)—O(6)W	88.2(3)	O(9)—Na(1)—O(5)W	79.4(2)
O(9)—Na(3)—O(6)W	87.8(3)	O(5)—Na(1)—O(6)W	79.6(3)
O(8)—Na(3)—O(6)W	80.0(3)	O(9)—Na(3)—O(5)W	78.3(3)
O(21)—Na(5)—O(4)W	85.6(3)	O(8)—Na(3)—O(5)W	79.4(3)
O(10)—Na(6)—O(19)	82.1(3)	O(5)W—Na(3)—O(6)W	73.8(3)
O(19)—Na(6)—O(3)W	93.7(3)	O(8)—Na(3)—O(9)	156.8(3)
O(4)—Na(6)—O(3)W	92.7(3)	O(12)—Na(7)—O(2)W	86.5(3)
C(6)—Na(6)—O(3)W	119.6(3)	O(4)—Na(6)—O(10)	52.3(3)
O(4)—Na(6)—O(19)	100.2(2)	C(6)—Na(6)—O(2)W	86.9(3)
O(4)—Na(6)—O(2)W	82.9(3)	O(10)—Na(6)—O(2)W	97.2(3)
Malonate Rings			
C(1)—C(2)—C(3)	116.1(8)	C(13)—C(14)—C(15)	119.1(8)
C(4)—C(5)—C(6)	121.3(9)	C(16)—C(17)—C(18)	120(1)
C(7)—C(8)—C(9)	121.7(9)	C(10—C(11)—C(12)	124(1)
O(17)—C(16)—C(17)	117(1)	O(24)—C(18)—C(17)	116(1)
O(20)—C(12)—C(11)	118(1)	O(21)—C(13)—C(14)	117.6(8)
O(14)—C(12)—C(11)	119.7(9)	O(22)—C(15)—C(14)	119.0(9)
O(14)—C(12)—O(20)	122.3(8)	O(16)—C(15)—O(22)	121.9(9)
O(17)—C(16)—O(23)	123(1)	O(15)—C(13)—C(14)	122.0(8)

obtained with the following hypotheses about the relaxation processes: isotropic (I), isotropic transverse (IT), transverse (T) and longitudinal (L). The computer fits were performed for all these cases. The best fit corresponds to the isotropic relaxation model at 293 K and respectively isotropic transverse at 4.2 K. That means the tensor γ describing relaxation in the Afanas'ev theory has identical x, y, z components at 293 K while the z component vanishes at 4.2 K. Figure 4 shows the spectral components following the Afanas'ev theory for the compound **1** at 4.2 and 293 K. The same behaviour was found by fitting the spectra of the compound **2**. The isotropic transverse relaxation is a good approximation for $|\pm 1/2\rangle$ Kramers doublet ($g_z = 2$ and $g_x = g_y = 6$). In the studied malonates the axial field parameter D is positive so, the $|\pm 1/2\rangle$ doublet lies lowest; at 4.2 K the doublet becomes dominant that explain the isotropic transverse structure of the relaxation tensor.

A fit employing the modified Bloch equations, suggested by Wickman *et al.* [15], to describe the electronic relaxation in terms of fluctuation of the effective hyperfine magnetic field, was also performed. In Fig. 5 the Mössbauer spectra together with the resulting fits for compound **2** are shown. The determined relaxation times (τ) for both compounds are of the order of 3, 4 ns. The results of the fit with both relaxation models are listed in Table 12.

A modified Marquardt–Levenberg fit [18] was used in the fitting programs. The quality of the fits was appreciated by using the χ^2 and MISFIT tests together with the linear correlation coefficient. The relaxation parameters γ and τ are comparable with those obtained for trisoxalatoferrate complexes [11–13]. The higher value of the isomer shift (about 0.4 mm/s) in the case of trismalonatoferrate complexes compared with the values reported for the trisoxalatoferrate [8,11] compounds (about 0.3 mm/s) indicates greater ionic bonding in malonic complexes. These values are characteristic for iron(III) in ^6S ground state (S 5/2, L 0). The iron(III) has a spherical symmetric distribution of electronic charge, conse-

Table 7. Possible hydrogen bonds (Å) and angles (°) for $[Na_3(FeMa_3)]_2 \cdot 8H_2O$ (**2**)

D—H···A[a]	D—H	D···A	H···A	Angle
O(3)W—H(3)WB···O(1)(*i*)	0.961(7)	2.902(9)	2.000(6)	155.6(6)
O(5)W—H(5)WB···O(6)W(*i*)	1.226(7)	2.96(1)	2.648(7)	92.2(4)
O(6)W—H(6)WA···O(24)(*i*)	0.816(7)	2.66(1)	1.961(8)	144.0(6)
O(6)W—H(6)WB···O(5)W(*i*)	0.990(7)	2.96(1)	1.971(7)	179.8(6)
O(7)W—H(7)WA···O(13)(*i*)	0.979(8)	2.90(1)	1.923(6)	178.9(5)
O(7)W—H(7)WA···O(19)(*i*)	0.979(8)	2.99(1)	2.376(7)	120.2(5)
O(7)W—H(7)WB···O(13)(*i*)	1.013(8)	2.90(1)	2.27(6)	118.8(5)
O(7)W—H(7)WB···O(19)(*i*)	1.013(8)	2.99(1)	1.978(7)	178.9(5)
O(8)W—H(8)WB···O(16)(*i*)	0.970(7)	2.926(9)	1.96(7)	179.9(5)
O(8)W—H(8)WB···O(17)(*i*)	0.970(7)	3.091(9)	2.654(6)	107.7(5)
O(1)W—H(1)WA···O(12)(*ii*)	0.887(8)	3.15(9)	2.879(7)	99.6(6)
O(5)W—H(5)WA···O(18)(*iii*)	0.822(7)	2.86(1)	2.055(7)	166.1(6)
O(1)W—H(1)WA···O(4)W(*iii*)	0.887(8)	2.82(1)	1.941(8)	171.9(6)
O(6)W—H(6)WB···O(2)(*iii*)	0.990(7)	3.121(9)	2.686(7)	106.9(5)
O(5)W—H(5)WB···O(2)(*iii*)	1.226(7)	2.83(1)	1.609(6)	176.4(5)
O(1)W—H(1)WB···O(2)W(*iv*)	0.615(7)	2.91(1)	2.305(7)	166.3(7)
O(2)W—H(2)WB···O(1)W(*v*)	0.908(7)	2.91(1)	2.024(7)	163.2(5)
O(8)W—H(8)WA···O(7)(*vi*)	0.969(6)	2.837(9)	1.868(6)	179.1(6)
O(6)W—H(6)WA···O(10)(*vii*)	0.816(7)	3.13(1)	2.701(7)	114.9(6)

[a]Equivalent positions: (*i*) x, y, z (*ii*) $-x+1, -y+1, -z+1$ (*iii*) $-x, -y+1, -z$ (*iv*) $x, y, z-1$ (*v*) $x, y, z+1$ (*vi*) $-x, -y+2, -z+1$ (*vii*) $-x, -y+1, -z+1$.

Table 8. Selected bond distances (Å) for $Na_3(FeMa_3) \cdot 8H_2O \cdot 1/2Sol$ (**3**)

Fe Site					
Fe—O(2)	1.982(3)				
Fe—O(9)	1.987(3)				
Fe—O(6)	1.999(3)				
Fe—O(5)	2.008(3)				
Fe—O(1)	2.010(3)				
Fe—O(10)	2.013(3)				
Na(1) Site			Na(2) Site		
Na(1)···O(12)	2.360(3)		Na(2)···O(4)W	2.356(3)	
Na(1)···O(2)W	2.369(3)		Na(2)···O(3)W	2.381(4)	
Na(1)···O(4)	2.435(3)		Na(2)···O(1)W($x, y, z+1$)	2.415(4)	
Na(1)···O(2)	2.458(2)		Na(2)···O(7; $-x+1, -y, -z+1$)	2.415(3)	
Na(1)···O(1)W	2.487(3)		Na(2)···O(2)W($x, y, z+1$)	2.520(3)	
Na(1)···O(3)	2.581(4)		Na(2)···O(7)	2.525(4)	
Na(3) Site			Na(4) Site		
Na(3)···O(4)W	2.338(4)		Na(4)···O(3)	2.369(4)	
Na(3)···O(2)S($x+1, y-1, z$)	2.400(4)		Na(4)···O(7)W	2.409(4)	
Na(3)···O(3)W($-x+1, -y, -z+1$)	2.424(3)		Na(4)···O(12)	2.461(3)	
Na(3)···O(6)W	2.441(5)		Na(4)···O(8)W	2.531(4)	
Na(3)···O(7)	2.478(3)		Na(4)···O(1)S	2.654(5)	
Na(5)···O(5)W	2.565(4)		Na(4)···O(2)S($-x-1, -y+1, -z$)	2.684(5)	
Malonate Rings					
C(2)—C(3)	1.514(5)	C(4)—C(5)	1.509(4)	C(8)—C(9)	1.515(5)
C(1)—C(2)	1.517(4)	C(5)—C(6)	1.515(4)	C(7)—C(8)	1.516(4)
O(3)—C(3)	1.234(4)	O(8)—C(4)	1.236(3)	O(11)—C(9)	1.240(4)
O(1)—C(1)	1.286(4)	O(6)—C(6)	1.284(3)	O(10)—C(9)	1.285(3)
O(2)—C(3)	1.291(4)	O(5)—C(4)	1.285(3)	O(9)—C(7)	1.287(3)
Solvate Molecule[a]					
C(1)S—C(2)S	1.48(9)	O(2)S—C(1)S	1.19(7)		
C(1)S—C(3)S	1.57(9)	O(1)S—C(1)S	1.16(9)		
C(3)S—C(3)S′	1.25(9)				

[a]Symmetry centre at $(-x-1; -y+1, -z)$.

Table 9. Selected bond angles (°) for $Na_3(FeMa_3)\cdot 8H_2O\cdot 1/2Sol$ (**3**)

Fe Site			
O(5)—Fe—O(6)	85.2(2)		
O(9)—Fe—O(10)	86.1(3)		
O(1)—Fe—O(10)	87.5(3)		
O(6)—Fe—O(10)	88.5(1)		
O(1)—Fe—O(6)	89.3(3)		
O(2)—Fe—O(5)	89.3(1)		
O(2)—Fe—O(9)	90.2(2)		
O(5)—Fe—O(9)	90.6(2)		
O(6)—Fe—O(9)	94.0(2)		
O(1)—Fe—O(5)	96.1(3)		
O(2)—Fe—O(10)	97.2(2)		
Na(1) Site		Na(2) Site	
O(2)—Na(1)—O(3)	51.8(2)	Na(3)—Na(2)—O(4)W	40.7(1)
O(4)—Na(1)—O(2)W	78.4(2)	Na(3)—Na(2)—O(7)	44.3(1)
O(3)—Na(1)—O(4)	81.0(2)	O(7)—Na(2)—O(4)W	85.1(2)
O(1)W—Na(1)—O(2)W	83.1(2)	O(7)—Na(2)—O(3)W	87.1(1)
O(3)—Na(1)—O(12)	84.5(2)	Na(3)—Na(2)—O(3)W	131.5(1)
O(2)—Na(1)—O(1)W	90.8(2)	O(3)W—Na(2)—O(4)W	172.2(1)
O(2)—Na(1)—O(12)	94.3(2)		
O(12)—Na(1)—O(1)W	98.5(3)		
O(2)—Na(1)—O(4)	86.0(2)		
Na(3) Site		Site	
O(4)—Na(3)—O(5)W	79.5(2)	O(1)S—Na(4)—C(3)S	48.0(2)
O(7)—Na(3)—O(5)W	80.5(2)	O(7)W—Na(4)—O(1)S	83.9(2)
O(7)—Na(3)—O(4)W	86.5(2)	O(7)W—Na(4)—O(8)W	86.7(2)
O(4)W—Na(3)—O(6)W	86.7(2)	O(12)—Na(4)—O(1)S	90.2(2)
O(5)W—Na(3)—O(6)W	107.9(3)	O(7)W—Na(4)—C(3)S	92.1(3)
O(7)—Na(3)—O(6)W	168.1(2)	O(12)—Na(4)—C(3)S	138.2(2)

Malonate Rings					
C(1)—C(2)—C(3)	117.8(5)	C(4)—C(5)—C(6)	116.8(4)	C(7)—C(8)—C(9)	117.3(5)
O(2)—C(3)—C(2)	118.2(4)	O(5)—C(4)—C(5)	119.0(4)	O(6)—C(6)—C(5)	118.7(4)
O(1)—C(1)—C(2)	119.0(6)	O(7)—C(6)—C(5)	119.2(5)	O(5)—C(4)—O(8)	121.9(4)
O(2)—C(3)—O(3)	121.4(5)	O(6)—C(6)—O(7)	122.0(3)	O(6)—C(6)—O(7)	122.0(3)

Solvate Molecule			
C(2)S—C(1)S—C(3)S	115.5(7)	O(2)S—C(1)S—C(2)S	106.0(6)
O(2)S—C(1)S—C(3)S	97.1(7)	O(1)S—C(1)S—O(2)S	140.3(9)
O(1)S—C(1)S—C(3)S	97.8(6)	Na(4)—C(3)S—C(1)S	103.8(5)
O(1)S—C(1)S—C(2)S	100.3(8)	Na(4)—O(1)S—C(1)S	105.8(5)

Table 10. Possible hydrogen bonds (Å) and angles (°) for $Na_3(FeMa_3)\cdot 8H_2O\cdot 1/2Sol$ (**3**)

D—H···A[a]	D—H	D···A	H···A	Angle
O(1)W—H(1)W(1)···O(5)(*i*)	1.03(6)	2.784(4)	1.77(6)	166(5)
O(2)W—H(2)W(2)···O(4)(*i*)	0.96(6)	3.038(4)	2.70(6)	101(3)
O(8)W—H(1)W(8)···O(12)(*i*)	0.92(8)	2.993(5)	2.80(7)	93(4)
O(1)W—H(2)W(1)···O(1)A(*ii*)	0.70(9)	2.932(6)	2.42(9)	174(9)
O(2)W—H(2)W(2)···O(5)W(*iii*)	0.96(6)	2.960(5)	2.04(5)	158(5)
O(2)W—H(1)W(2)···O(10)(*ii*)	0.99(5)	2.851(4)	1.88(5)	167(4)
O(8)W—H(1)W(8)···O(11)(*iii*)	0.92(8)	2.781(5)	1.87(8)	170(6)
O(8)W—H(2)W(8)···O(6)W(*iv*)	1.22(7)	3.028(6)	2.091(8)	130(5)
O(7)W—H(1)W(7)···O(8)(*v*)	0.88(6)	2.773(5)	1.96(7)	151(7)
O(8)W—H(2)W(8)···O(2)A(*vi*)	1.22(7)	3.010(6)	2.69(9)	92(4)

[a] Equivalent positions: (*i*) x, y, z (*ii*) $-x, -y+1, -z$ (*iii*) $x, y, z-1$ (*iv*) $-x, -y, -z$ (*v*) $x-1, y+1, z$ (*vi*) $-x-1, -y+1, -z$.

Table 11. Dihedral angles between weighted least-squares planes at the iron sites together with the closest Fe···Fe distance

Compound	*a*/*b* (°)	*a*/*c* (°)	*b*/*c* (°)	Fe···Fe (Å)
1[i]	96.7(1)	93.9(1)	106.1(1)	6.77(1)
2 Fe(1)[ii]	104.7(2)	113.3(2)	59.2(2)	6.60(1)
2 Fe(2)[iii]	95.3(3)	84.3(2)	105.7(1)	—
3[iv]	97.7(1)	67.7(1)	121.2(1)	6.86(1)

[i] *a* FeO(1)C(1)C(2)C(3)O(3), *b* FeO(5)C(4)C(5)C(6)O(7), *c* Fe O(9)C(7)C(8)C(9)O(11).
[ii] *a* Fe(1)O(1)C(1)C(2)C(3)O(2), *b* Fe(1)O(3)C(4)C(5)C(6)O(4), *c* Fe(1)O(5)C(7)C(8)C(9)O(6).
[iii] *a* Fe(2)O(13)C(10)C(11)C(12)O(14), *b* Fe(2)O(15)C(13)C(14)C(15)O(16), *c* Fe(2)O(17)C(16)C(17)C(18)O(18).
[iv] *a* FeO(1)C(1)C(2)C(3)O(2), *b* FeO(5)C(4)C(5)C(6)O(6), *c* FeO(9)C(7)C(8)C(9)O(10).

Table 12. Mössbauer parameters for compounds **1** and **2** following the various models

Compound	Model[a]	Temp (K)	IS[b] (mm/s)	QS (mm/s)	LW (mm/s)	γ (s/mm)	τ (ns)	χ^2
1	Lorentzian	293	0.44(1)	—	1.95(3)	—	—	2.88
	Lorentzian	4.2	0.45(1)	—	2.40(3)	—	—	3.65
	Afanas'ev (I)[a]	293	0.43(1)	−0.06(2)	0.89(1)	0.013(2)	—	1.34
	Afanas'ev (IT)[a]	4.2	0.40(1)	−0.08(2)	0.88(1)	0.024(2)	—	1.25
	Wickman	293	0.41(1)	−0.06(3)	0.89(1)	—	4.60(4)	1.38
	Wickman	4.2	0.35(1)	−0.11(3)	0.88(1)	—	4.11(4)	1.18
2	Lorentzian	293	0.41(1)	—	1.92(3)	—	—	4.52
	Lorentzian	4.2	0.43(1)	—	2.38(3)	—	—	6.31
	Afanas'ev (I)[a]	293	0.38(1)	0.06(2)	0.72(1)	0.019(2)	—	1.32
	Afanas'ev (IT)[a]	4.2	0.34(1)	−0.07(2)	0.71(1)	0.032(2)	—	1.28
	Wickman	293	0.47(1)	0.07(3)	0.72(1)	—	2.88(4)	1.12
	Wickman	4.2	0.34(1)	−0.07(3)	0.71(1)	—	2.97(4)	1.08

[a] I = isotropic, IT = isotropic transverse.
[b] Isomer shift referred to metallic iron at room temperature.

quently the main contribution to QS comes from the lattice. In order to obtain more detailed information about the QS a theoretical electric field gradient calculation has been performed [19]. A value close to 0.1 mm/s was found for QS in relatively good agreement with those given by the fit within the relaxation models.

Since the relaxation time is practically temperature independent, the observed broadening in the Mössbauer spectra can be attributed to spin–spin relaxation phenomena. The results are in agreement with the slightly distorted octahedral iron(III) sites, with the Fe···Fe distances (less than 7 Å) as well as with the parameters reported for trisoxalatoferrate compounds [11,13]. The Mössbauer lineshape does not change basically going from oxalato to malonato groups in the studied alkali iron(III) compounds.

In conclusion the deviations in $Fe(III)O_6$ octahedral geometry, by using malonato instead of oxalato ligands, are scarcely reflected in Mössbauer parameters. In both oxalato and malonato derivatives the sites $Fe(III)O_6$ are connected by a complex net of hydrogen bonding due to water molecules, together with a solvate molecule in **3**. The hydrogen bonding modulates the closest $FeO_6\cdots FeO_6$ distance which is sensibly the same. This explains the scarce variation in strength of the relaxation phenomena in oxalato and malonato compounds.

Acknowledgements—Financial support from the University of Venice, MURST, and CNR-Rome is gratefully acknowledged.

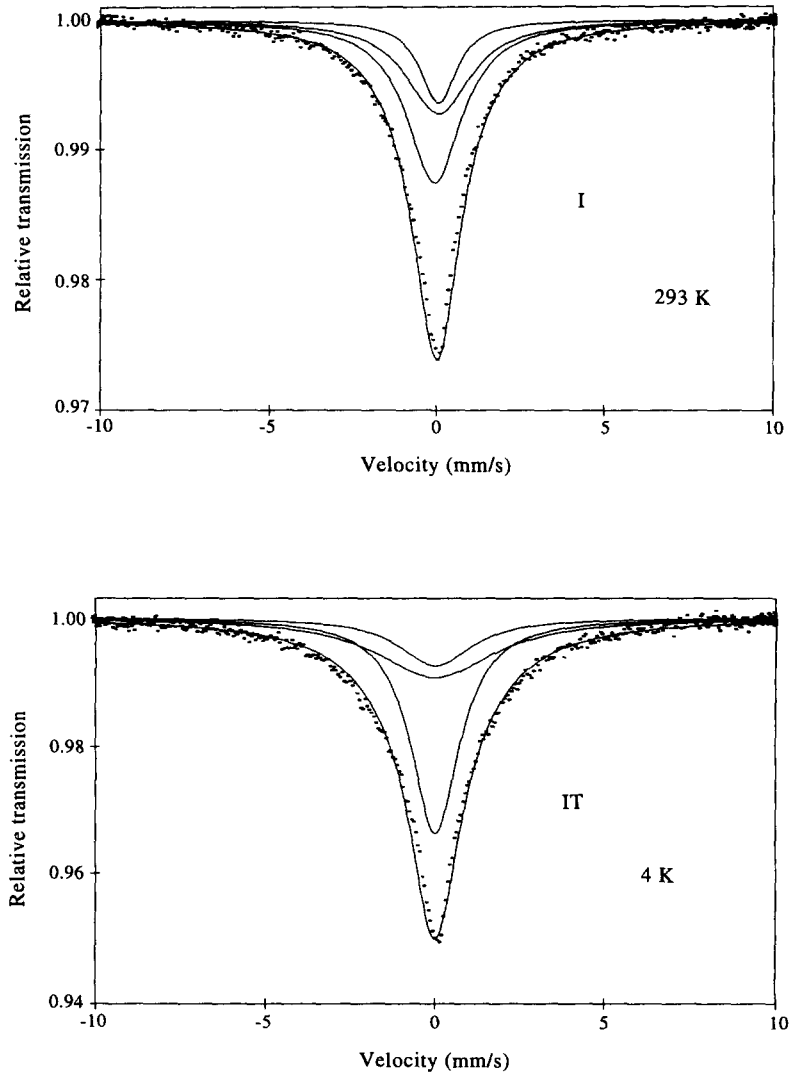

Fig. 4. Mössbauer spectra at 293 and 4.2 K for the compound **1**, following Afanas'ev theory.

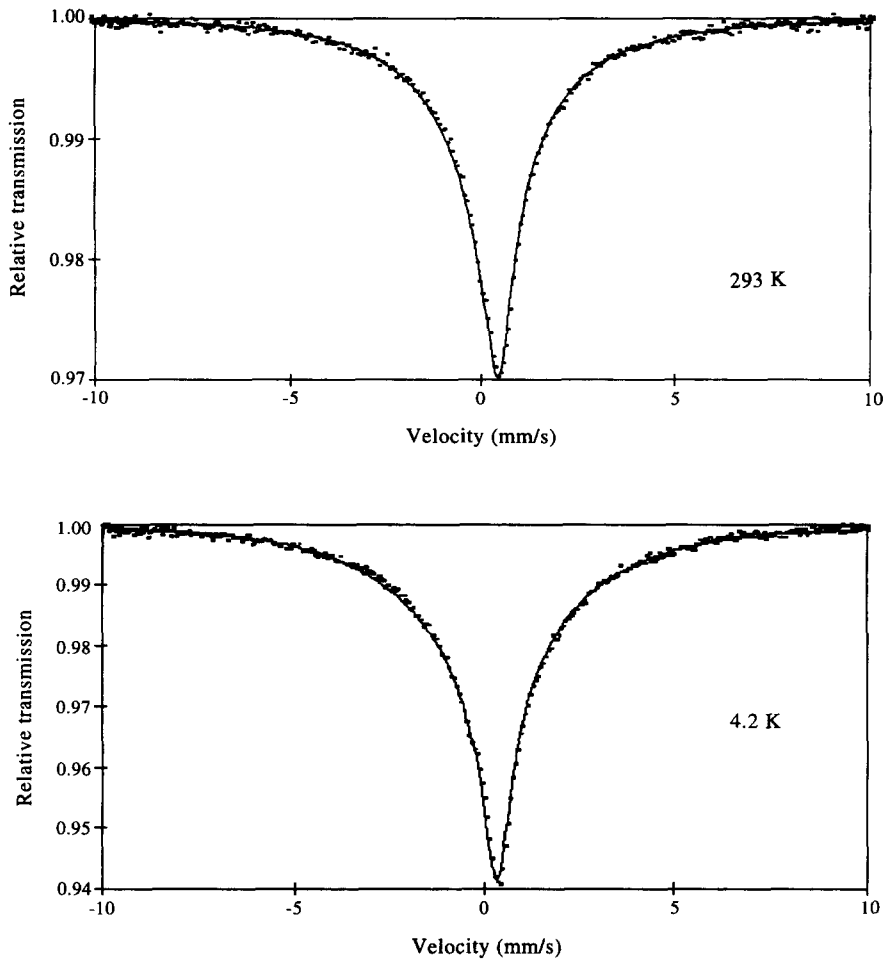

Fig. 5. Mössbauer spectra at 293 and 4.2 K for the compound **2**, following Wickman theory.

REFERENCES

1. Adamson, A. W., Waltz, W. L., Zinato, E., Watts, D. W., Fleischauer, P. D. and Lindholm, R. D., *Chem. Rev.*, 1968, **68,** 541.
2. Kosar, J., *Light Sensitive Systems*, Wiley, New York (1965).
3. Gmelius Handbuech, *System Numeer* 53, Teil B-Lieferung 1930, **3,** 536.
4. Jorgensen, Che. Klixbull, *Inorganic Complexes*, p. 97. Academic Press, London and New York (1963).
5. Dziobkowski, Che. T., Wbrobleski, J. T. and Brown, D. B., *Inorg. Chem.*, 1981, **20,** 671.
6. Farago, M. E. and Amirhaeri, S., *Inorg. Chim. Acta*, 1984, **81,** 205.
7. Abras, A., De Jesus Filho, M. F. and Braga, M. M., *Thermochim. Acta*, 1986, **101,** 135.
8. Bassi, P. S., Randhawa, B. S. and Kaur, S., *Hyperfine Interactions*, 1986, **28,** 745.
9. Lanjewar, R. B., Waditwar, A. M. and Garg, A. N., *J. Radioanal. & Nucl. Chem.*, 1988, **125,** 75.
10. Collison, D. and Powell, A. K., *Inorg. Chem.*, 1990, **29,** 4735.
11. Barb, D., Diamandescu, L. and Mihăilă-Tărăbăşanu, D., *J. Physique*, 1976, **37,** C6–113.
12. Barb, C., Diamandescu, L. and Mihăilă-Tărăbăşanu, D., *Chem. Phys.*, 1979, **44,** 239.
13. Barb, D., Diamandescu, L. and Mihăilă-Tărăbăşanu, D., *J. Physique*, 1980, **41,** C1–227.
14. Afanas'ev, A. M. and Gorobchenco, V. D., Report IAE-2215, Moscow 1972, *Zh. Eksp. Teor. Fiz.*, 1974, **66,** 1406.
15. Wickman, H. H., Klein, M. P. and Shirley, D. A., *Phys. Rev. B.*, 1966, 152, 345.
16. Heidrich, W., *Z. Phys.*, 1970, **230,** 418.
17. Morgan, C. H., *Acta Crystallogr.*, 1967, **23,** 239.
18. Weber, M., *Turbo Pascal Tools*, Braunschwieg (Vieweg) 1988.
19. Constantinescu, S., IFM, Bucharest, private communication, 1997.